

## Synthesis and Characterization of Cationic Tungsten(V) Methylidyne

Edwin F. van der Eide,<sup>†</sup> Warren E. Piers,<sup>\*†</sup> Masood Parvez,<sup>†</sup> and Robert McDonald<sup>‡</sup>*Department of Chemistry, University of Calgary, 2500 University Drive NW, Calgary, Alberta, Canada T2N 1N4, and X-ray Structure Laboratory, Department of Chemistry, University of Alberta, Edmonton, Alberta, Canada T6G 2G2*

Received June 22, 2006

Cationic tungsten(V) methylidyne  $[L_4W(X)\equiv CH]^+[B(C_6F_5)_4]^-$  [ $L = PMe_3, 0.5dmpe$  ( $dmpe = Me_2PCH_2CH_2PMe_2$ ),  $X = Cl, OSO_2CF_3$ ] have been prepared in high yield by a one-electron oxidation of the neutral tungsten(IV) methylidyne  $L_4W(X)\equiv CH$  with  $[Ph_3C]^+[B(C_6F_5)_4]^-$ . The ease and reversibility of the one-electron oxidation of  $L_4W(X)\equiv CH$  were demonstrated by cyclic voltammetry in tetrahydrofuran ( $E_{1/2} \approx -0.68$  to  $-0.91$  V vs Fc). The paramagnetic  $d^1$  ( $S = 1/2$ ) complexes were characterized in solution by electron spin resonance ( $g = 2.023$ – $2.048$ , quintets due to coupling to  $^{31}P$ ) and NMR spectroscopy and Evans magnetic susceptibility measurements ( $\mu = 2.0$ – $2.1 \mu_B$ ). Single-crystal X-ray diffraction showed that the cationic methylidyne are structurally similar to the neutral precursor methylidyne. In addition, the neutral  $(PMe_3)_4W(Cl)\equiv CH$  was deprotonated with a strong base at the trimethylphosphine ligand to afford  $(PMe_3)_3(Me_2PCH_2)W\equiv CH$ , a tungsten(IV) methylidyne complex that features a (dimethylphosphino)methyl ligand.

## Introduction

Although examples of complexes containing a terminal methylidyne ligand,  $L_nM\equiv CH$ , have been known for some time,<sup>1</sup> their occurrence remains scarce, and examples are restricted to the group 6 metals Mo and W. Two general classes (based on d electron count) have been identified. The Schrock,<sup>2</sup> Chisholm,<sup>3</sup> and Cummins<sup>4</sup> groups have each produced variants on the  $d^0 X_3M\equiv CH$  motif (where X is a bulky anionic donor), while both the Templeton<sup>5</sup> and Schrock<sup>1,6</sup> groups have introduced  $d^2$  methylidyne, of which

Schrock and co-workers' original methylidyne  $(L)_4W(X)\equiv CH$  are the most studied. The reactivity of  $(L)_4M(X)\equiv CH$  has been widely explored, particularly their reactions with electrophiles.<sup>6–8</sup> Furthermore, Hopkins et al. have extensively probed their electronic and vibrational structure<sup>9</sup> in connection with studies aimed at incorporating the  $X-W\equiv CH$  axis into conjugated metallopolymers.<sup>10</sup>

In light of these materials' applications, the redox behavior of alkylidyne and methylidyne of this general formula is of interest. In this context, Hopkins et al. have prepared the paramagnetic  $d^1$  benzylidyne complex  $[(dmpe)_2W(Br)\equiv CPh]^- [PF_6]^+$  ( $dmpe = Me_2PCH_2CH_2PMe_2$ ) via one-electron oxidation of the neutral  $d^2$  benzylidyne using the tropylium cation as the oxidizing agent.<sup>11</sup> Isolated paramagnetic alkylidyne are rare species,<sup>12</sup> and they possess the capacity for dimerization,<sup>7a</sup> a situation that would presumably be

\* To whom correspondence should be addressed. E-mail: wpiers@ucalgary.ca. Phone: 403-220-5746. Fax: 403-289-9488.

<sup>†</sup> University of Calgary.

<sup>‡</sup> University of Alberta.

- (1) (a) Sharp, P. R.; Holmes, S. J.; Schrock, R. R.; Churchill, M. R.; Wasserman, H. J. *J. Am. Chem. Soc.* **1981**, *103*, 965.
- (2) (a) Seidel, S. W.; Schrock, R. R.; Davis, W. M. *Organometallics* **1998**, *17*, 1058. (b) Schrock, R. R.; Seidel, S. W.; Möscher-Zanetti, N. C.; Dobbs, D. A.; Shih, K.-Y.; Davis, W. M. *Organometallics* **1997**, *16*, 5195.
- (3) Chisholm, M. H.; Folting, K.; Hoffman, D. M.; Huffman, J. C. *J. Am. Chem. Soc.* **1984**, *106*, 6794.
- (4) (a) Peters, J. C.; Odom, A. L.; Cummins, C. C. *Chem. Commun.* **1997**, 1995. (b) Greco, J. B.; Peters, J. C.; Baker, T. A.; Davis, W. M.; Cummins, C. C. *J. Am. Chem. Soc.* **2001**, *123*, 5003. (c) Agapie, T.; Diaconescu, P. L.; Cummins, C. C. *J. Am. Chem. Soc.* **2002**, *124*, 2412.
- (5) (a) Enriquez, A. E.; White, P. S.; Templeton, J. L. *J. Am. Chem. Soc.* **2001**, *123*, 4992. (b) Jamison, G. M.; Bruce, A. E.; White, P. S.; Templeton, J. L. *J. Am. Chem. Soc.* **1991**, *113*, 5057.
- (6) Holmes, S. J.; Clark, D. N.; Turner, H. W.; Schrock, R. R. *J. Am. Chem. Soc.* **1982**, *104*, 6322.

- (7) (a) Holmes, S. J.; Schrock, R. R.; Churchill, M. R.; Wasserman, H. J. *Organometallics* **1984**, *3*, 476. (b) Manna, J.; Geib, S. J.; Hopkins, M. D. *Angew. Chem., Int. Ed. Engl.* **1993**, *32*, 858.
- (8) van der Eide, E. F.; Piers, W. E.; Romero, P. E.; Parvez, M.; McDonald, R. *Organometallics* **2004**, *23*, 314.
- (9) (a) Manna, J.; Kuk, R. J.; Dallinger, R. F.; Hopkins, M. D. *J. Am. Chem. Soc.* **1994**, *116*, 9793. (b) Manna, J.; Dallinger, R. F.; Miskowski, V. M.; Hopkins, M. D. *J. Phys. Chem. B* **2000**, *104*, 10928. (c) Da Re, R. E.; Hopkins, M. D. *Coord. Chem. Rev.* **2005**, *249*, 1396.
- (10) (a) Manna, J.; Geib, S. J.; Hopkins, M. D. *J. Am. Chem. Soc.* **1992**, *114*, 9199. (b) See also: Mayr, A.; Yu, M. P. Y.; Yam, V. W.-W. *J. Am. Chem. Soc.* **1999**, *121*, 1760.
- (11) Manna, J.; Gilbert, T. M.; Dallinger, R. F.; Geib, S. J.; Hopkins, M. D. *J. Am. Chem. Soc.* **1992**, *114*, 5870.

exacerbated in the less sterically protected parent methylidyne compounds, where even diamagnetic examples dimerize.<sup>3,5b</sup> Nonetheless, in the context of our continuing interest in the reactions of archetypal organometallic fragments with electrophiles,<sup>8,13</sup> we discovered that the reaction of Schrock and co-workers' methylidyne ( $(L)_4W(X)\equiv CH$  ( $L = PMe_3$  or  $0.5dmpe$ ;  $X = Cl$  or  $OTf$ ) with the trityl borate reagent  $[Ph_3C][B(C_6F_5)_4]^{14}$  leads to facile one-electron oxidation to the cationic  $d^1$  methylidyne  $[(L)_4W(X)\equiv CH][B(C_6F_5)_4]^+$ , the first monomeric paramagnetic methylidyne complexes to be characterized.

## Experimental Section

**Reagents and General Procedures.** All operations were performed under a purified Ar atmosphere using glovebox or vacuum-line techniques. Toluene, hexanes, and tetrahydrofuran (THF) solvents were dried and purified by passing through activated alumina and Q5 columns.<sup>15</sup> Acetonitrile and dichloromethane were dried over  $CaH_2$  and distilled under reduced pressure. Diethyl ether and pentane were dried over Na/benzophenone and distilled under reduced pressure. Methylidyne  $(PMe_3)_4W(Cl)\equiv CH$  (**1a**) and  $(dmpe)_2W(Cl)\equiv CH$  (**1b**) were prepared as described in the literature,<sup>6</sup> while the compound  $(dmpe)_2W(OTf)\equiv CH$  (**1c**) was prepared by treatment of **1b** with  $Me_3SiOTf$ .<sup>7b</sup> Isotopomers  $(PMe_3)_4W(Cl)\equiv^{13}CH$  (**1a-<sup>13</sup>C-1a**) and  $(PMe_3)_4W(Cl)\equiv CD$  (**1a-d<sub>1</sub>**) and derivatives were prepared by reacting  $(PMe_3)_4WCl_2$ <sup>16</sup> with  $Al(^{13}CH_3)_3$  or  $Al(CD_3)_3$  instead of unlabeled  $Al(CH_3)_3$ .

**Instrumentation.**  $^1H$ ,  $^2H\{^1H\}$ ,  $^{11}B$ ,  $^{13}C$ ,  $^{19}F$ , and  $^{31}P$  NMR spectra were collected on a Bruker AC-200, AMX-300, or DRX-400 spectrometer in dry,  $O_2$ -free  $C_6D_6$ ,  $C_7D_8$ ,  $CD_2Cl_2$ , THF- $d_8$ ,  $C_6D_5Br$ , or  $CD_3CN$ . Chemical shifts are given in ppm relative to residual solvent signals for  $^1H$  and  $^{13}C$  NMR spectra.  $^{11}B$ ,  $^{19}F$ , and  $^{31}P$  NMR spectra were referenced to external  $Et_2O\cdot BF_3$ ,  $C_6F_6$ , and 85%  $H_3PO_4$ , respectively. Electrochemical studies were carried out using an EG&G model 283 potentiostat in conjunction with a three-electrode cell. The auxiliary electrode was a Pt wire, the pseudo-reference electrode a Ag wire, and the working electrode a Pt disk (1.6 mm diameter). Solutions (in THF or acetonitrile) were 1 mM in the tungsten compound and 0.1 M in  $[^nBu_4N][PF_6]$  as the supporting electrolyte. IR spectra were recorded as KBr pellets on a Nicolet Nexus 470 FT-IR spectrometer in the range 4000–400  $cm^{-1}$ . Solution magnetic moments were determined at 298 K in THF/THF- $d_8$  (3:1) according to the Evans method.<sup>17</sup> Electron spin resonance (ESR) spectra were recorded on a Bruker EMX 113 spectrometer. WINEPR SimFonia<sup>18</sup> was used to simulate the spectra, and Lorentzian line shapes were used in the

simulations;  $g_{iso}$  values, hyperfine coupling constants, and line widths can be found in Table 2. The  $g_{iso}$  values of the radicals were calculated using the field/frequency ratio of each sample. UV–visible spectra were obtained on a Cary 100 Bio spectrophotometer operating in double-beam mode. Elemental analyses were performed by Olivera Blagojevic and Roxanna Smith (University of Calgary).

**Synthesis of  $[(PMe_3)_4W(Cl)\equiv CH]^+[B(C_6F_5)_4]^-$  (**2a**).**  $(PMe_3)_4W(Cl)\equiv CH$  (0.153 g, 0.285 mmol) and  $[Ph_3C]^+[B(C_6F_5)_4]^-$  (0.265 g, 0.287 mmol) were placed in a 50-mL flask attached to a swivel-frit assembly, and toluene (20 mL) was condensed onto the yellow solids at  $-78^\circ C$ . The orange suspension was allowed to warm to room temperature, during which a color change to green was observed, as well as the formation of a green precipitate. The supernatant had a yellow color. The suspension was stirred at room temperature for another 30 min, after which the green solids were collected on the frit and washed with several portions of toluene. Drying in vacuo gave a bright-green powder, which was isolated. Yield: 0.320 g (0.263 mmol, 93%). Crystals of **2a**· $C_6D_6$  suitable for X-ray analysis were obtained from an NMR tube reaction between  $(PMe_3)_4W(Cl)\equiv CH$  and 1 equiv of  $[Ph_3C]^+[B(C_6F_5)_4]^-$  in  $C_6D_6$ , from which **2a** precipitated as a green oil. Dark-green prismatic crystals had grown on the oil/ $C_6D_6$  interface after 30 min.  $^1H$  NMR (THF- $d_8$ , 400 MHz, 300 K):  $\delta$  8.2 (v br,  $\Delta\nu_{1/2} \approx 2500$  Hz, 36H,  $CH_3$ ),  $W\equiv CH$  not observed, probably very broad.  $^{19}F$  NMR (THF- $d_8$ , 282.4 MHz, 300 K):  $\delta$   $-132.6$  (*o*-F),  $-164.7$  (*p*-F),  $-168.2$  (*m*-F).  $^{11}B$  NMR (THF- $d_8$ , 128.2 MHz, 300 K):  $\delta$   $-17.4$  ( $B(C_6F_5)_4$ ).  $^{31}P\{^1H\}$  and  $^{13}C\{^1H\}$  NMR spectra are silent.  $\mu$  (THF, 298 K) = 2.0  $\mu_B$ . IR: 3011 (w), 2985 (w), 2920 (w), 2850 (w), 2804 (w), 1643 (m), 1515 (s), 1464 (s), 1420 (m), 1292 (m), 1275 (m), 1087 (s), 980 (s), 951 (s), 775 (m), 756 (m), 684 (m), 662 (m). Anal. Calcd for  $C_{37}H_{37}BClF_{20}P_4W$ : C, 36.56; H, 3.07. Found: C, 36.69; H, 3.01.

**Synthesis of  $[(dmpe)_2W(Cl)\equiv CH]^+[B(C_6F_5)_4]^-$  (**2b**).**  $(dmpe)_2W(Cl)\equiv CH$  (0.150 g, 0.282 mmol) and  $[Ph_3C]^+[B(C_6F_5)_4]^-$  (0.260 g, 0.282 mmol) were placed in a 50-mL flask attached to a swivel-frit assembly, and toluene (20 mL) was condensed onto the yellow solids at  $-78^\circ C$ . The orange suspension was allowed to warm to room temperature, during which a color change to light green was observed, as well as the formation of a green precipitate. The supernatant had a light-yellow color. The suspension was stirred at room temperature for another 30 min, after which the green solids were collected on the frit and washed with several portions of toluene. Drying in vacuo afforded a yellow/green powder, which was isolated. Yield: 0.320 g (0.264 mmol, 94%). Light-green crystals of **2b** suitable for X-ray analysis were grown by slow evaporation of solvent from a  $CH_2Cl_2$  solution of **2b**.  $^1H$  NMR ( $CD_2Cl_2$ , 400 MHz, 300 K):  $\delta$  2.71 (br,  $\Delta\nu_{1/2} \approx 160$  Hz, 12H,  $CH_3$ ), 1.34 (br,  $\Delta\nu_{1/2} \approx 160$  Hz, 12H,  $CH_3$ ),  $-11$  (v br,  $\Delta\nu_{1/2} \approx 1600$  Hz, 1H,  $W\equiv CH$ ).  $^1H$  NMR ( $C_6D_5Br$ , 400 MHz, 300 K):  $\delta$  2.20 (br, 12H,  $-CH_3$ ), 1.10 (br, 12H,  $-CH_3$ ),  $-11$  (v br, 1H,  $W\equiv CH$ ). Resonances for the methylene protons could not be observed; these are probably buried underneath the methyl resonances as broad lines.  $^{11}B$  NMR ( $CD_2Cl_2$ , 128.2 MHz, 300 K):  $\delta$   $-17.3$  ( $B(C_6F_5)_4$ ).  $^{19}F$  NMR ( $CD_2Cl_2$ , 282.4 MHz, 300 K):  $\delta$   $-132.5$  (*o*-F),  $-163.5$  (*p*-F),  $-167.3$  (*m*-F).  $^{19}F$  NMR ( $C_6D_5Br$ , 282.4 MHz, 300 K):  $\delta$   $-133.2$  (*o*-F),  $-163.4$  (*p*-F),  $-167.2$  (*m*-F).  $^{31}P\{^1H\}$  and  $^{13}C\{^1H\}$  NMR spectra are silent.  $\mu$  (THF, 298 K) = 2.1  $\mu_B$ . IR: 2977 (w), 2938 (w), 2907 (w), 1643 (m), 1515 (s), 1465 (s), 1421 (m), 1372 (w), 1292 (m), 1275 (m), 1090 (s), 977 (s), 951 (m), 934 (m), 895 (m), 777 (m), 758 (m), 686 (m), 664 (m). Anal. Calcd for  $C_{37}H_{33}BClF_{20}P_4W$ : C, 36.68; H, 2.75. Found: C, 36.93; H, 2.60.

- (12) (a) Xue, W.-M.; Chan, M. C. W.; Mak, T. C. W.; Che, C.-M. *Inorg. Chem.* **1997**, *36*, 6437. (b) Felixberger, J. K.; Kiprof, P.; Herdtweck, E.; Herrmann, W. A.; Jakobi, R.; Gütllich, P. *Angew. Chem., Int. Ed. Engl.* **1989**, *28*, 334. (c) Lemos, M. A. N. D. A.; Pombeiro, A. J. L.; Hughes, D. L.; Richards, R. L. *J. Organomet. Chem.* **1992**, *434*, C6.  
 (13) For example, see: (a) Spence, R. E. v. H.; Piers, W. E.; Sun, Y.; Parvez, M.; MacGillivray, L. R.; Zaworotko, M. J. *Organometallics* **1998**, *17*, 2459. (b) Cook, K. S.; Piers, W. E.; McDonald, R. J. *Am. Chem. Soc.* **2002**, *124*, 5411.  
 (14) Chien, J. C. W.; Tsai, W.-M.; Rausch, M. D. *J. Am. Chem. Soc.* **1991**, *113*, 8570.  
 (15) Pangborn, A. B.; Giardello, M. A.; Grubbs, R. H.; Rosen, R. K.; Timmers, F. J. *Organometallics* **1996**, *15*, 1518.  
 (16) Sharp, P. R.; Bryan, J. C.; Mayer, J. M. *Inorg. Synth.* **1990**, *28*, 326.  
 (17) (a) Evans, D. F. *J. Chem. Soc.* **1959**, 2003. (b) Schubert, E. M. *J. Chem. Educ.* **1992**, *69*, 62. (c) Grant, D. H. *J. Chem. Educ.* **1995**, *72*, 39.  
 (18) WINEPR SimFonia, version 1.25; Bruker Analytische Messtechnik GmbH: Karlsruhe, Germany, 1996.

**Table 1.** Data Collection and Structure Refinement Details for **2a**·C<sub>6</sub>D<sub>6</sub>, **2b**, and **3**

	<b>2a</b> ·C <sub>6</sub> D <sub>6</sub>	<b>2b</b>	<b>3</b>
formula	C <sub>43</sub> H <sub>37</sub> D <sub>6</sub> BClF <sub>20</sub> P <sub>4</sub> W	C <sub>37</sub> H <sub>33</sub> BClF <sub>20</sub> P <sub>4</sub> W	C <sub>13</sub> H <sub>36</sub> P <sub>4</sub> W
fw	1299.80	1211.62	500.15
cryst syst	triclinic	orthorhombic	monoclinic
space group	<i>P</i> $\bar{1}$	<i>Pca</i> 2 <sub>1</sub>	<i>C2/c</i>
<i>a</i> , Å	13.667(2)	27.5938(18)	30.889(11)
<i>b</i> , Å	14.036(3)	11.9743(8)	8.924(2)
<i>c</i> , Å	15.665(2)	13.3408(9)	15.485(6)
$\alpha$ , deg	64.577(8)	90	90
$\beta$ , deg	68.486(9)	90	94.582(17)
$\gamma$ , deg	73.640(8)	90	90
<i>V</i> , Å <sup>3</sup>	2497.2(7)	4408.0(5)	4255(2)
<i>Z</i>	2	4	8
<i>T</i> , K	123	193	173
$\lambda$ , Å	0.710 73	0.710 73	0.710 73
$\rho_{\text{calc}}$ , g cm <sup>-3</sup>	1.729	1.826	1.562
<i>F</i> (000)	1274	2364	1984
$\mu$ , mm <sup>-1</sup>	2.601	2.940	5.72
cryst size, mm <sup>3</sup>	0.10 × 0.08 × 0.07	0.68 × 0.26 × 0.07	0.16 × 0.12 × 0.05
transm factors	0.781–0.839	0.2397–0.8206	0.462–0.763
$\theta$ range, deg	3.0–30.0	2.25–26.38	3.2–27.5
data/restraints/param	14484/0/656	8964/0/597	4857/0/177
GOF	1.06	1.007	1.04
R1 [ <i>I</i> > 2 $\sigma$ ( <i>I</i> )]	0.037	0.0243	0.032
wR2 (all data)	0.076	0.0548	0.076
residual density, e Å <sup>-3</sup>	1.04 and –1.07	1.260 and –0.322	0.99 and –1.15

**Synthesis of [(dmpe)<sub>2</sub>W(OTf)≡CH]<sup>+</sup>[B(C<sub>6</sub>F<sub>5</sub>)<sub>4</sub>]<sup>-</sup>·PhCH<sub>3</sub> (**2c**·PhCH<sub>3</sub>).** (dmpe)<sub>2</sub>W(OTf)≡CH (0.111 g, 0.172 mmol) and [Ph<sub>3</sub>C]<sup>+</sup>[B(C<sub>6</sub>F<sub>5</sub>)<sub>4</sub>]<sup>-</sup> (0.160 g, 0.173 mmol) were placed in a 50-mL flask attached to a swivel-frit assembly, and toluene (20 mL) was condensed onto the yellow solids at –78 °C. The orange suspension was allowed to warm to room temperature, during which clumps of a green material precipitated. These clumps were sonicated into a green powder. After the green solids were stirred at room temperature for another 30 min, they were collected on the frit and washed with several portions of toluene. Drying in vacuo afforded a green powder, which was isolated. Yield: 0.199 g (0.150 mmol, 82%). <sup>1</sup>H NMR (THF-*d*<sub>8</sub>, 400 MHz, 300 K):  $\delta$  7.21–7.05 (m, 5H, CH<sub>3</sub>C<sub>6</sub>H<sub>5</sub>), 5.28 (br,  $\Delta\nu_{1/2} \approx 400$  Hz, 12H, CH<sub>3</sub>), 2.30 (s, 3H, CH<sub>3</sub>C<sub>6</sub>H<sub>5</sub>), –0.3 (br, 8H, CH<sub>2</sub>), –1.23 (br,  $\Delta\nu_{1/2} \approx 350$  Hz, 12H, CH<sub>3</sub>), –10.2 (v br,  $\Delta\nu_{1/2} \approx 1100$  Hz, 1H, W≡CH). <sup>19</sup>F NMR (THF-*d*<sub>8</sub>, 282.4 MHz, 300 K):  $\delta$  –75.2 (br, OSO<sub>2</sub>CF<sub>3</sub>), –130.9 (*o*-F), –163.1 (*p*-F), –166.6 (*m*-F). <sup>11</sup>B NMR (THF-*d*<sub>8</sub>, 128.2 MHz, 300 K):  $\delta$  –17.4 (B(C<sub>6</sub>F<sub>5</sub>)<sub>4</sub>). <sup>31</sup>P{<sup>1</sup>H} and <sup>13</sup>C{<sup>1</sup>H} NMR spectra are silent.  $\mu$  (THF, 298 K) = 2.1  $\mu_B$ . IR: 2992 (w), 2908 (w), 1643 (w), 1515 (m), 1464 (s), 1423 (w), 1322 (w), 1235 (w), 1207 (m), 1087 (m), 1025 (m), 980 (s), 949 (m), 775 (w), 756 (w), 684 (w), 662 (w), 635 (m). Anal. Calcd for C<sub>45</sub>H<sub>41</sub>BF<sub>23</sub>O<sub>3</sub>P<sub>4</sub>SW: C, 38.13; H, 2.92. Found: C, 37.61; H, 2.92.

**Synthesis of (PMe<sub>3</sub>)<sub>3</sub>(Me<sub>2</sub>PCH<sub>2</sub>)W≡CH (**3**).** (PMe<sub>3</sub>)<sub>4</sub>W(Cl)≡CH (0.311 g, 0.580 mmol) and KCH<sub>2</sub>Ph (0.101 g, 0.776 mmol) were placed in a 25-mL flask attached to a swivel-frit assembly. THF (10 mL) was condensed onto the solids at –78 °C, and the mixture was allowed to warm to room temperature. The dark-red solution was stirred for 30 min at room temperature, after which the volatiles were removed in vacuo. Pentane (5 mL) was condensed onto the residue at –78 °C, and the mixture was sonicated at room temperature for 5 min, after which the volatiles were removed in vacuo. Pentane (20 mL) was condensed onto the residue at –78 °C, and filtering at room temperature afforded a yellow solution. Removal of the pentane in vacuo afforded a yellow/orange solid, which was isolated. Yield: 0.240 g (0.480 mmol, 83%). Yellow crystals of **3** suitable for X-ray analysis were grown by cooling a saturated pentane solution of **3** to –35 °C for several days. <sup>1</sup>H NMR (C<sub>6</sub>D<sub>6</sub>, 400 MHz, 300 K):  $\delta$  8.72 (ddtt, <sup>3</sup>J<sub>HP</sub> = 5.2, 2.3, and 2.2

Hz, <sup>4</sup>J<sub>HH</sub> = 0.9 Hz, <sup>2</sup>J<sub>HW</sub> = 74 Hz, <sup>1</sup>J<sub>CH</sub> = 125 Hz, 1H, W≡CH), 1.54 (dd, <sup>2</sup>J<sub>HP</sub> = 8.1 Hz, <sup>4</sup>J<sub>HP</sub> = 1.3 Hz, 6H, WCH<sub>2</sub>P(CH<sub>3</sub>)<sub>2</sub>), 1.52 (ps t, 18H, PMe<sub>3</sub>), 1.49 (d, <sup>2</sup>J<sub>HP</sub> = 6.9 Hz, 9H, PMe<sub>3</sub>), –1.26 (ddtt, <sup>2</sup>J<sub>HP</sub> = 4.1 Hz, <sup>3</sup>J<sub>HP</sub> = 13.0 and 2.8 Hz, <sup>4</sup>J<sub>HH</sub> = 0.9 Hz, 2H, WCH<sub>2</sub>P(CH<sub>3</sub>)<sub>2</sub>). <sup>1</sup>H NMR (THF-*d*<sub>8</sub>, 300 MHz, 300 K):  $\delta$  8.13 (m, 1H, W≡CH), 1.60 (d, 9H, PMe<sub>3</sub>), 1.53 (dd, overlapping, 6H, WCH<sub>2</sub>P(CH<sub>3</sub>)<sub>2</sub>), 1.51 (ps t, 18H, PMe<sub>3</sub>), –1.58 (ps tt, 2H, WCH<sub>2</sub>P(CH<sub>3</sub>)<sub>2</sub>). <sup>1</sup>H NMR (C<sub>7</sub>D<sub>8</sub>, 400 MHz, 300 K):  $\delta$  8.58 (ddtt, 1H, W≡CH), 1.53 (dd, 6H, WCH<sub>2</sub>P(CH<sub>3</sub>)<sub>2</sub>), 1.50 (ps t, 18H, PMe<sub>3</sub>), 1.49 (d, overlapping, 9H, PMe<sub>3</sub>), –1.35 (ddtt, 2H, WCH<sub>2</sub>P(CH<sub>3</sub>)<sub>2</sub>). <sup>1</sup>H NMR (C<sub>7</sub>D<sub>8</sub>, 400 MHz, 185 K):  $\delta$  8.97 (br, 1H, W≡CH), 1.83 (br, 6H, 1 CH<sub>3</sub> of PMe<sub>3</sub>), 1.74 (br, 6H, 1 CH<sub>3</sub> of PMe<sub>3</sub>), 1.58 (br d, 6H, WCH<sub>2</sub>P(CH<sub>3</sub>)<sub>2</sub>), 1.45 (br, 9H, PMe<sub>3</sub>), 1.09 (br, 6H, 1 CH<sub>3</sub> of PMe<sub>3</sub>), –1.16 (br, 2H, WCH<sub>2</sub>P(CH<sub>3</sub>)<sub>2</sub>). <sup>31</sup>P{<sup>1</sup>H} NMR (C<sub>6</sub>D<sub>6</sub>, 161.8 MHz, 300 K):  $\delta$  –14.0 (dt, <sup>2</sup>J<sub>PP(cis)</sub> = 13.5 Hz, <sup>2</sup>J<sub>PP(pseudo-trans)</sub> = 26.5 Hz, <sup>1</sup>J<sub>PW</sub> = 339 Hz, 1P, PMe<sub>3</sub>), –31.0 (ps t, <sup>2</sup>J<sub>PP(cis)</sub> = 13.5 and 14.0 Hz, <sup>1</sup>J<sub>PW</sub> = 281 Hz, 2P, PMe<sub>3</sub>), –52.8 (dt, <sup>2</sup>J<sub>PP(cis)</sub> = 14.0 Hz, <sup>2</sup>J<sub>PP(pseudo-trans)</sub> = 26.5 Hz, <sup>1</sup>J<sub>PW</sub> = 249 Hz, 1P, WCH<sub>2</sub>PMe<sub>2</sub>). <sup>13</sup>C{<sup>1</sup>H} NMR (C<sub>6</sub>D<sub>6</sub>, 100.5 MHz, 300 K):  $\delta$  264.8 (ddt, W≡CH), 28.6 (ps t, 2 PMe<sub>3</sub>), 26.9 (d ps q, PMe<sub>3</sub>), 19.8 (d ps q, WCH<sub>2</sub>P(CH<sub>3</sub>)<sub>2</sub>), –23.1 (ddt, WCH<sub>2</sub>P(CH<sub>3</sub>)<sub>2</sub>). IR: 2959 (m), 2927 (m), 2901 (s), 2798 (w), 1415 (m), 1292 (m), 1279 (m), 930 (s), 872 (m), 840 (m), 704 (m), 652 (m). Anal. Calcd for C<sub>13</sub>H<sub>36</sub>P<sub>4</sub>W: C, 31.22; H, 7.25. Found: C, 29.99; H, 7.62. This was the best result of several analyses; the compound was quite sensitive and also contained variable amounts (<5%) of an impurity believed to be (Me<sub>3</sub>P)<sub>4</sub>WH<sub>4</sub>, based on reported NMR data for this compound.<sup>19</sup>

**Single-Crystal X-ray Analyses.** Crystals of **2a**·C<sub>6</sub>D<sub>6</sub> and **2b** were coated with Paratone 8277 oil, those of **3** with perfluoropolyalkyl ether (1600 cSt), and mounted on a glass fiber. Measurements for **2a**·C<sub>6</sub>D<sub>6</sub> and **3** were made on a Nonius Kappa CCD diffractometer (University of Calgary) and those for **2b** on a Bruker PLATFORM/SMART 1000 CCD diffractometer (University of Alberta), using graphite-monochromated Mo K $\alpha$  radiation for all measurements. Table 1 gives further details, and the crystallographic data (CIF) are available as Supporting Information. The CCDC contains the supplementary crystallographic data for the crystal

(19) Lyons, D.; Wilkinson, G. *J. Chem. Soc., Dalton Trans.* **1985**, 587.

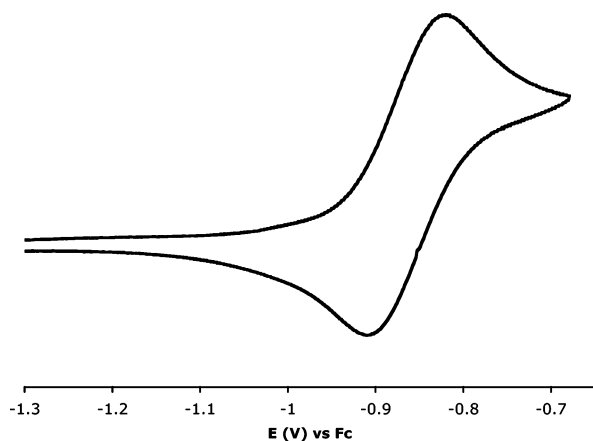


**Figure 1.** Cyclic voltammogram (scan rate  $10 \text{ mV s}^{-1}$ ) of  $1 \text{ mM } \mathbf{1a}$  in THF at room temperature with  $0.1 \text{ M } [n\text{-Bu}_4\text{N}][\text{PF}_6]$  as the supporting electrolyte.

structures reported in this paper (CCDC 605925, **2a**· $\text{C}_6\text{D}_6$ ; CCDC 605926, **2b**; CCDC 605927, **3**). These data can be obtained, free of charge, via [www.ccdc.cam.ac.uk/conts/retrieving.html](http://www.ccdc.cam.ac.uk/conts/retrieving.html) (or from the Cambridge Crystallographic Data Centre, 12 Union Road, Cambridge CB2 1EZ, U.K.; fax 44-1223-336033; or e-mail [deposit@ccdc.cam.ac.uk](mailto:deposit@ccdc.cam.ac.uk)).

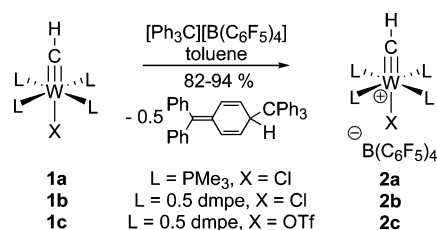
## Results and Discussion

### One-Electron Oxidation of Tungsten(IV) Methylidyne.

Methylidyne  $\text{L}_4\text{W}(\text{X})\equiv\text{CH}$  ( $\text{L}, \text{X} = \text{PMe}_3, \text{Cl}, \mathbf{1a}$ ;  $0.5\text{dmpe}, \text{Cl}, \mathbf{1b}$ ;  $0.5\text{dmpe}, \text{OTf}, \mathbf{1c}$ ) can be reversibly oxidized, as was found by cyclic voltammetry in THF (Figure 1;  $[\text{W}] = 1 \text{ mM}, 0.1 \text{ M } [n\text{-Bu}_4\text{N}][\text{PF}_6]$  electrolyte,  $\text{Cp}_2\text{Fe}$  as the internal standard). One-electron oxidations to the  $\text{W}^{\text{V}}$  radical cations  $[\text{L}_4\text{W}(\text{X})\equiv\text{CH}]^+$  ( $\mathbf{1}^+$ ) were found in all cases, with  $E_{1/2}$  values of  $-0.88, -0.91,$  and  $-0.68 \text{ V vs Fc}$  ( $[\text{Cp}_2\text{Fe}]^{+1/0}$  couple) for the couples  $\mathbf{1a}^+/\mathbf{1a}, \mathbf{1b}^+/\mathbf{1b},$  and  $\mathbf{1c}^+/\mathbf{1c}$ , respectively. These data indicate that the denticity of the phosphine ligand has a negligible effect on the  $E_{1/2}$  value, whereas substitution of Cl for OTf significantly increases the redox potential by ca.  $0.20 \text{ V}$ . This can be attributed to a greater positive charge on W in  $\mathbf{1c}$  vs  $\mathbf{1b}$  due to the more weakly coordinating or electron-withdrawing nature of  $\text{OTf}^-$  vs  $\text{Cl}^-$ . The  $d^1$  cations  $\mathbf{1}^+$  generated in the cyclic voltammetry experiments were found to be persistent in a THF solution because reversible oxidations were observed also at low scan rates. The redox potentials of the methylidyne complexes are comparable to the potentials found for tungsten(IV) dialkyl complexes  $\text{Cp}_2\text{WRR}'$  (ca.  $-0.80$  to  $-0.64 \text{ V vs Fc}$ , MeCN solvent,  $[\text{Et}_4\text{N}][\text{ClO}_4]$  electrolyte), as determined by Cooper and co-workers.<sup>20</sup>

Clean chemical oxidation of methylidyne  $\mathbf{1}$  is readily achieved by reaction with the trityl cation  $\text{Ph}_3\text{C}^+$  ( $E_{1/2} = -0.11 \text{ V vs Fc}$  in MeCN<sup>21</sup>). NMR tube reactions of yellow  $\mathbf{1}$  with 1 equiv of  $[\text{Ph}_3\text{C}]^+[\text{B}(\text{C}_6\text{F}_5)_4]^-$  in  $\text{C}_6\text{D}_6$  result in the precipitation of green oils or solids, leaving a light-yellow supernatant (Scheme 1). In each case,  $^1\text{H}$  NMR spectroscopy reveals the absence of W-containing products in solution,

### Scheme 1



and multiplet resonances at (among others) 4.93, 5.91, and 6.43 ppm clearly indicate the formation of the known dimer resulting from head-to-tail coupling of the trityl radical.<sup>22</sup> The oxidation reaction also goes very cleanly in THF- $d_8$ , in which the products stay dissolved. Although Cooper's  $\text{W}^{\text{V}}$  cations  $[\text{Cp}_2\text{WRR}']^+$  undergo  $\text{H}^\bullet$  radical abstraction from an alkyl  $\alpha\text{-C}$  in the presence of trityl radicals to form triphenylmethane, the methylidyne cations do not react with trityl radicals under any conditions we tried.

$\text{B}(\text{C}_6\text{F}_5)_4^-$  salts **2** (Scheme 1) were synthesized on a preparative scale by the reaction of  $\mathbf{1}$  with 1 equiv of  $[\text{Ph}_3\text{C}]^+[\text{B}(\text{C}_6\text{F}_5)_4]^-$  in toluene. The ion pairs are insoluble in toluene and precipitate as green microcrystalline materials in the course of the reaction. Filtration and washing of the precipitate with toluene removes the soluble organic byproduct and affords **2a** (green) and **2b** (bright green/yellow) as analytically pure powders in ca. 90% yield. Triflate derivative **2c** (green) is obtained in a yield of 82%, and its combustion analysis and  $^1\text{H}$  NMR spectrum suggest that approximately 1 equiv of toluene is retained in the isolated solid material. In the solid state at  $-35 \text{ }^\circ\text{C}$ , the ion pairs are indefinitely stable, and also after days at room temperature, there is no sign of decomposition. Ion pairs **2** are soluble in polar solvents, such as halobenzenes,  $\text{CH}_2\text{Cl}_2$ , THF, and  $\text{CH}_3\text{CN}$ . While dmpe-containing **2b** and **2c** are stable in all of these solvents, **2a** decomposes within 24 h in  $\text{CH}_2\text{Cl}_2$  and  $\text{CH}_3\text{CN}$  to unknown products. The solutions are highly  $\text{O}_2$ -sensitive; opening them to air results in a disappearance of the green or yellow color and decomposition to unidentified products. Complexes **2** are the first stable, monomeric paramagnetic methylidyne to be isolated. Churchill et al. synthesized a formally tungsten(V) phosphinomethylidyne<sup>7a</sup> by the reaction of  $\mathbf{1a}$  with  $\text{AlCl}_3/\text{C}_2\text{Cl}_6$ , but the product is dimeric and diamagnetic and the methylidyne proton is somehow lost in the reaction.

Single-crystal X-ray analysis of  $\mathbf{2a}\cdot\text{C}_6\text{D}_6$  (Figure 2) corroborates its formulation as a cationic tungsten(V) methylidyne complex. The methylidyne and chloride ligands are disordered (Cl and C atoms were included with 0.5 occupancy factors on either side of the  $\text{WP}_4$  plane), which does not justify a discussion of metrical data associated with the  $\text{Cl}-\text{W}\equiv\text{CH}$  axis. The same type of disorder was found to be operative in the crystal structure of the parent  $\mathbf{1a}$ ,<sup>23</sup> determined by Churchill and co-workers. In both  $\mathbf{1a}$  and  $\mathbf{2a}$ , the  $\text{W}(\text{PMe}_3)_4$  part is ordered, with the  $\text{PMe}_3$  ligands situated alternately above and below the least-squares  $\text{WP}_4$  plane.

(20) Asaro, M. F.; Cooper, S. R.; Cooper, N. J. *J. Am. Chem. Soc.* **1986**, *108*, 5187.

(21) Connelly, N. G.; Geiger, W. E. *Chem. Rev.* **1996**, *96*, 877.

(22) McBride, J. M. *Tetrahedron* **1974**, *30*, 2009.

(23) Churchill, M. R.; Rheingold, A. L.; Wasserman, H. J. *Inorg. Chem.* **1981**, *20*, 3392.

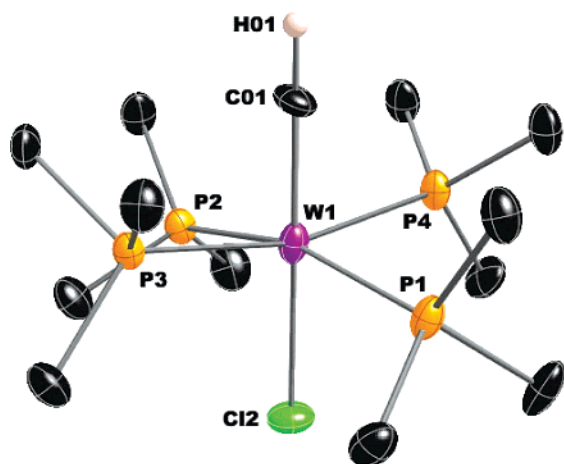


**Figure 2.** Crystallmaker depiction (50% probability thermal ellipsoids) of the molecular structure of **2a**·C<sub>6</sub>D<sub>6</sub>. The anion, cocrystallized C<sub>6</sub>D<sub>6</sub>, and H atoms, except the methylidyne H (arbitrary radius), are omitted for clarity, and the disorder of the methylidyne and chloride ligands is not shown. Selected bond lengths (Å): W1–P1, 2.5430(9); W1–P2, 2.5347(9); W1–P3, 2.5280(8); W1–P4, 2.5301(8). Selected bond angles (deg): P1–W1–P2, 165.39(3); P3–W1–P4, 164.70(3).

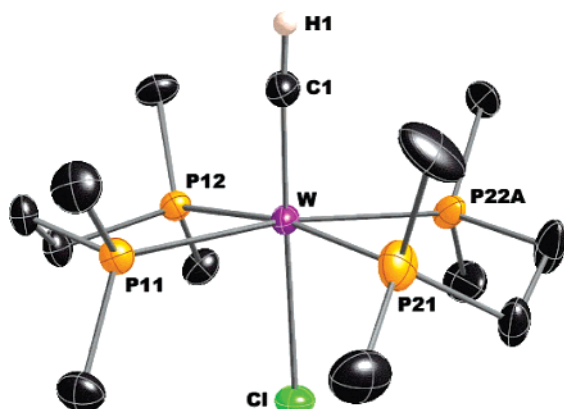


**Figure 3.** Crystallmaker depiction (50% probability thermal ellipsoids) of the molecular structure of **2b**. The anion and H atoms, except the methylidyne H (arbitrary radius), are omitted for clarity, and the disorder in the P21/P22 dmpe ligand is not shown. Selected bond lengths (Å): W–C1, 1.776(5); W–Cl, 2.5561(12); W–P11, 2.5198(9); W–P12, 2.5018(8); W–P21, 2.5069(11); W–P22A, 2.471(3); C1–H1, 0.88(7). Selected bond angles (deg): Cl–W–Cl, 176.63(16); P11–W–P12, 79.91(3); P21–W–P22A, 77.72(5); P11–W–P21, 94.34(3); P12–W–P22A, 107.02(5).

Interestingly, in going from the neutral **1a** to the cationic **2a**, the average W–P bond length [ $d(W-P)_{av}$ ] increases from 2.467(2) to 2.534(6) Å, i.e., by 2.7%. While the opposite trend might have been expected on the basis of an increased electrophilicity of the W atom, the increase in  $d(W-P)_{av}$  reflects the diminished W  $d-(P-C)$   $\sigma^*$  back-donation<sup>24</sup> in the W<sup>V</sup>  $d^1$  product compared to the W<sup>IV</sup>  $d^2$  starting material.

Methylidyne/chloride ligand disorder is absent in the crystal structure of **2b**, displayed in Figure 3, although in this case one of the dmpe ligands is disordered. This disorder was satisfactorily dealt with by placing several of the dmpe atoms in the two positions A and B with occupancy factors

of 0.75 and 0.25, respectively (in Figure 3, the A position is displayed). Such a dmpe disorder is the rule rather than the exception for (dmpe)<sub>2</sub>W complexes and has been discussed elsewhere.<sup>25</sup> The methylidyne hydrogen H1 was located and refined; the linearity of the Cl–W≡CH unit is evidenced by W–C1–H1 and Cl–W–C1 angles of 175(4)° and 176.6(2)°, respectively. The W–Cl bond length in **2b** is 2.556(1) Å, shorter than the 2.606(3) Å determined<sup>26</sup> for **1b**, while the W≡C length of 1.776(5) Å is statistically almost identical with the length of 1.797(10) Å in **1b**.<sup>26</sup> This shortening of the W–Cl bond upon oxidation is expected for the electron-donating chloride ligands. Again, the average W–P bond length is ca. 0.06 Å longer in **2b** than in **1b**. The W–P and W≡C bond lengths found here for **2b** compare very well to those found for [(dmpe)<sub>2</sub>W(Br)≡CPh]<sup>+</sup>[PF<sub>6</sub>]<sup>–</sup>, a closely related tungsten(V) benzylidyne complex reported by Hopkins and co-workers.<sup>11</sup>

Magnetic moments of **2** in a THF solution were determined by the Evans method<sup>17</sup> to be 2.0–2.1  $\mu_B$ , relatively close to the spin-only value of 1.7  $\mu_B$  expected for a complex with a single unpaired electron. As a consequence, the NMR spectra are paramagnetically broadened. The <sup>1</sup>H NMR spectrum of **2a** in THF-*d*<sub>8</sub> shows a very broad ( $\Delta\nu_{1/2} \approx 2500$  Hz) signal at 8.2 ppm for the 36 equivalent PME<sub>3</sub> protons, which sharpens slightly upon heating of the sample to 335 K and which broadens upon cooling. The single methylidyne proton, which may be broadened to an even larger extent because of its closer proximity to the W center, could not be observed. <sup>2</sup>H NMR spectroscopy on **2a-d**<sub>1</sub>, deuterated at the methylidyne position, also afforded a featureless spectrum. Likewise, paramagnetic broadening prevented the observation of signals in the <sup>13</sup>C and <sup>31</sup>P NMR spectra. In contrast, resonances for the B(C<sub>6</sub>F<sub>5</sub>)<sub>4</sub><sup>–</sup> anion in the <sup>19</sup>F and <sup>11</sup>B NMR spectra are sharp and are located at unperturbed chemical shift values, which suggests that the diamagnetic anion is solvent-separated from the paramagnetic cation. NMR spectra of **2a** in other solvents such as C<sub>6</sub>D<sub>5</sub>Br and CD<sub>2</sub>Cl<sub>2</sub> are very similar to those recorded in THF-*d*<sub>8</sub>. The <sup>1</sup>H NMR resonances for **2b** and **2c** are much less broadened than those of **2a**, although <sup>13</sup>C and <sup>31</sup>P NMR spectra are still featureless. For example, the methylidyne protons of **2b** and **2c** are now visible at ca. –9 to –11 ppm in the <sup>1</sup>H NMR spectra as broad ( $\Delta\nu_{1/2} \approx 1100$ – $1500$  Hz) resonances, just distinguishable from the baseline. Furthermore, the two sets of inequivalent methyl protons (**2b**,  $\delta$  2.71 and 1.34 ppm; **2c**,  $\delta$  +5.28 and –1.23 ppm) have widths at half-height of only 160–400 Hz (cf. 2500 Hz for **2a**).

Complexes **2** were further characterized in a THF solution ([**2**]  $\approx 1$  mM) by variable-temperature X-band ESR spectroscopy. Simple symmetric spectra were obtained for each of the complexes; those of **2b** at temperatures of 295 and 220 K are displayed in Figure 4. The  $g_{iso}$  value of 2.048 indicates that the radical is W-based, and hyperfine coupling

(24) (a) Orpen, A. G.; Connelly, N. G. *Organometallics* **1990**, *9*, 1206. (b) The average P–C bond length, which is 1.818(6) Å in **2a**·C<sub>6</sub>D<sub>6</sub> and 1.832(11) Å in **1a**, exhibits the expected trend for a lower population of antibonding P–C  $\sigma^*$  orbitals in the former complex, but caution should be used in interpreting this observation because of the larger estimated standard deviations associated with these bonds.

(25) Ménoret, C.; Spasojevic-de Biré, A.; Quy Dao, N.; Cousson, A.; Kiat, J.-M.; Manna, J. D.; Hopkins, M. D. *J. Chem. Soc., Dalton Trans.* **2002**, 3731.

(26) Manna, J.; Mlinar, L. A.; Kuk, R. J.; Dallinger, R. F.; Geib, S. J.; Hopkins, M. D. In *Transition Metal Carbyne Complexes*; Kreissl, F. R., Ed.; Kluwer Academic Publishers: Dordrecht, The Netherlands, 1993; pp 75–77.

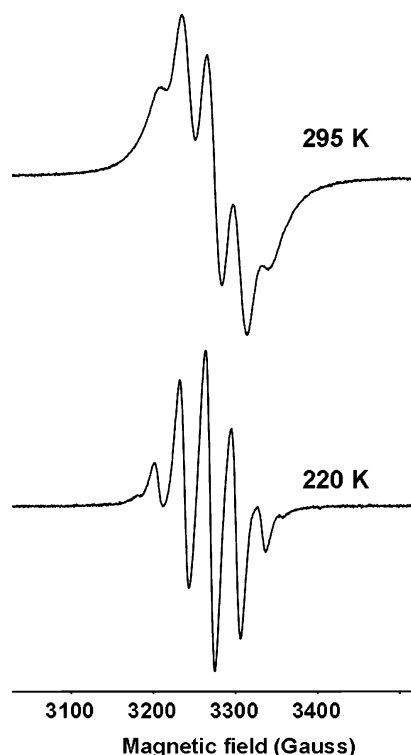


**Figure 4.** Variable-temperature X-band ESR spectra of **2b** in THF.

**Table 2.** ESR Parameters<sup>a</sup> for Tungsten(V) Methylidyne Radicals in THF

	<i>T</i> (K)	<i>g</i> <sub>iso</sub>	line width	<i>a</i> <sup>31P</sup>	<i>a</i> <sup>183W</sup>	<i>a</i> <sup>13C</sup>
<b>2a</b>	290	2.0234	20.0	34.5	52	<i>b</i>
	200	2.0259	10.0	35.0	52	8.0
<b>2b</b>	295	2.0479	23.5	31.0	45	<i>b</i>
	200	2.0503	9.5	31.5	45	8.0
<b>2c</b>	295	2.0444	17.0	31.0	45	<i>b</i>
	200	2.0478	7.8	31.5	45	8.0

<sup>a</sup> Line widths and HFCCs are in gauss. Estimated standard deviations:  $\pm 0.0001$  for *g*<sub>iso</sub>,  $\pm 0.5$  G for line width, *a*<sup>31P</sup>, *a*<sup>13C</sup>, and *a*<sup>1H</sup>,  $\pm 2$  G for *a*<sup>183W</sup>.  
<sup>b</sup> Coupling is hardly visible because of broad lines.

to the four equivalent P atoms (<sup>31P</sup>, *I* = 1/2, 100%, *a*<sup>31P</sup> = 31 G) is observed. Because of significant line broadening at ambient temperature, the quintet pattern is highly distorted, but the line width decreases upon cooling of the sample, until at 220 K an almost regular quintet is obtained. At these low temperatures, the hyperfine coupling to W (<sup>183W</sup>, *I* = 1/2, 14%, *a*<sup>183W</sup> = 45 G) also becomes visible, as weak satellites flank the outer lines of the main *I* = 0 signal. The observed ESR spectra of **2** were successfully simulated; hyperfine coupling constants (HFCCs), *g*<sub>iso</sub> values, and line widths extracted from these simulations are listed in Table 2. Notably, even though the singly occupied molecular orbitals of **2** are *d*<sub>xy</sub> orbitals oriented perpendicular to the X–W≡CH axes, coupling to the methylidyne C atoms could also be discerned and simulated in low-temperature spectra of the isotopomers [<sup>13C</sup>]**2** (*a*<sup>13C</sup> ≈ 8 G; see Figure 5). This suggests that probably hyperfine coupling to the chloride (for **2a** and **2b**) and to the methylidyne proton also occurs, but the line widths are too high to resolve the corresponding HFCCs. Several other W d<sup>1</sup> complexes have been previously characterized by ESR spectroscopy, but the majority are of

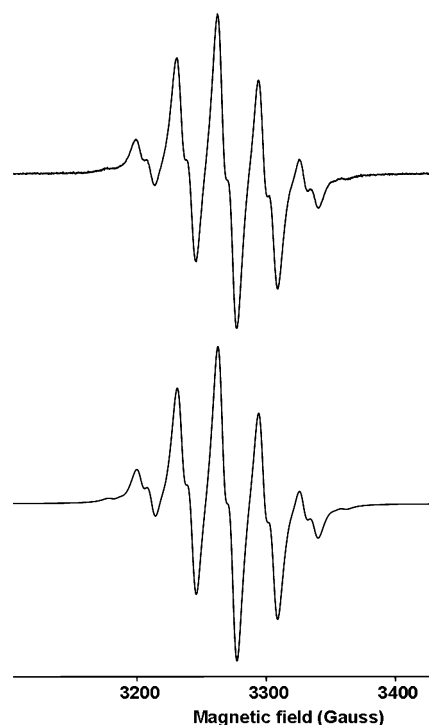


**Figure 5.** Experimental (top) and simulated ESR spectra of [<sup>13C</sup>]**2c**•PhCH<sub>3</sub> in THF at 200 K.

the bent metallocene type [Cp<sub>2</sub>WRR']<sup>+</sup> and bear little relevance to the octahedral methylidyne studied here. However, a somewhat related phosphine ligated W<sup>V</sup> radical is [WCl<sub>2</sub>(H)<sub>2</sub>(PMe<sub>3</sub>)<sub>4</sub>]<sup>+</sup> (*g*<sub>iso</sub> = 2.00, *a*<sup>31P</sup> = 22 and 25 G), reported by Sharp and Frank.<sup>27</sup>

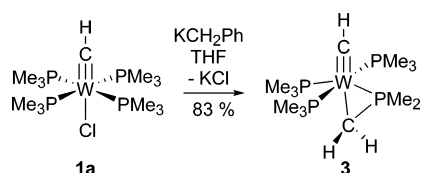
The UV–visible spectra of compounds **2** were recorded in C<sub>6</sub>H<sub>5</sub>F, THF, and MeCN solutions, in concentration ranges of 0.3–1.0 mM, and exhibited three bands in the visible range of 300–500 nm with  $\epsilon$  values of ca. 1000 M<sup>-1</sup> cm<sup>-1</sup>. These are the expected bands based on the electronic structure treatment presented by Da Re and Hopkins for a d<sup>1</sup> complex of the general formula L<sub>5</sub>M≡CR<sup>9c</sup> and can be assigned as *d*<sub>xy</sub> →  $\pi^*$ ,  $\pi$  → *d*<sub>xy</sub>, and  $\pi$  →  $\pi^*$  transitions in a [ $\pi$ M≡CR]<sup>4</sup>[*d*<sub>xy</sub>]<sup>1</sup> ground-state configuration.

**Attempted Deprotonation of 2a.** While Schrock et al. originally reported that the neutral d<sup>2</sup> methylidyne **1** are not susceptible to deprotonation using alkyllithium or alkoxide bases in aromatic solvents,<sup>7a</sup> we felt that the cationic d<sup>1</sup> systems described above might be more acidic. Somewhat surprisingly, treatment of **2a** with a range of strong bases, including lithium diisopropylamide (LDA), benzylpotassium (KBn), and the phosphazene base [(Me<sub>2</sub>N)<sub>3</sub>P=N]<sub>3</sub>P=N<sup>t</sup>Bu,<sup>28</sup> led to reduction rather than deprotonation, and the major product recovered was the neutral d<sup>2</sup> methylidyne **1a**; the

(27) (a) Sharp, P. R.; Frank, K. G. *Inorg. Chem.* **1985**, *24*, 1808. (b) See also: Saboonchian, V.; Wilkinson, G.; Hussain-Bates, B.; Hursthouse, M. B. *Polyhedron* **1991**, *10*, 595.

(28) (a) Swesinger, R.; Schlemper, H.; Hasenfratz, C.; Willaredt, J.; Dambacher, T.; Breuer, T.; Ottaway, C.; Fletschinger, M.; Boele, J.; Fritz, H.; Putzas, D.; Rotter, H. W.; Bordwell, F. G.; Satish, A. V.; Ji, G.-Z.; Peters, E.-M.; Peters, K.; von Schnering, H. G.; Walz, L. *Liebigs Ann. Chem.* **1996**, 1055. (b) Swesinger, R.; Schlemper, H. *Angew. Chem., Int. Ed. Engl.* **1987**, *26*, 1167. (c) Swesinger, R.; Hasenfratz, C.; Schlemper, H.; Walz, L.; Peters, E.-M.; Peters, K.; von Schnering, H. G. *Angew. Chem., Int. Ed. Engl.* **1993**, *32*, 1361.

Scheme 2



products associated with the reductant were not fully identified.<sup>29</sup> Another, less symmetrical, diamagnetic W-containing product was also observed in minor amounts, and the proportion of this species was observed to increase when larger excesses of base were employed. Indeed, it was the dominant product when **2a** was treated with a full 2 equiv of either LDA or KBN, suggesting that this product arises from deprotonation of **1a** after one-electron reduction of **2a**.

Accordingly, it was determined that a methyl group of a coordinated trimethylphosphine ligand in **1a** can be deprotonated smoothly in THF by LDA or KBN, yielding the yellow, highly pentane-soluble product  $(\text{PMe}_3)_3(\text{Me}_2\text{PCH}_2)\text{W}\equiv\text{CH}$  (**3**; Scheme 2), a neutral tungsten(IV) methylidyne complex that contains a formally monoanionic (dimethylphosphino)methyl ligand.<sup>30</sup> With LDA, the reaction proceeded very slowly, requiring more than 1 week to achieve >80% conversion, but the more basic KBN furnishes **3** in 30 min in an equally clean reaction. Extraction with pentane, followed by evaporation of the volatiles, affords **3** in 83% isolated yield. The identity of **3** was confirmed by X-ray analysis (vide infra) and multinuclear NMR spectroscopy. The incipient  $\text{PCH}_2^-$  group that results from deprotonation of **1a** apparently displaces  $\text{Cl}^-$  in a fast intramolecular nucleophilic substitution reaction. It should be noted that **1a** itself does not engage in bimolecular nucleophilic substitution reactions with  $\text{LiMe}$ ,  $\text{LiCH}_2\text{CMe}_3$ ,  $\text{LiBET}_3\text{H}$ , or  $\text{LiOCMe}_3$ , as reported by Schrock and co-workers.<sup>7a</sup>

The solid-state structure of **3** is displayed in Figure 6. Although the asymmetric unit consists of one molecule of **3**, the molecule, nevertheless, possesses near- $C_s$  symmetry. The geometry around W is perhaps best described as a highly distorted octahedron in which C1, P2, and P4 occupy more or less regular positions and C2, P1, and P3 are distorted from their regular positions. For P3, this distortion reduces unfavorable steric interactions between the methyl groups

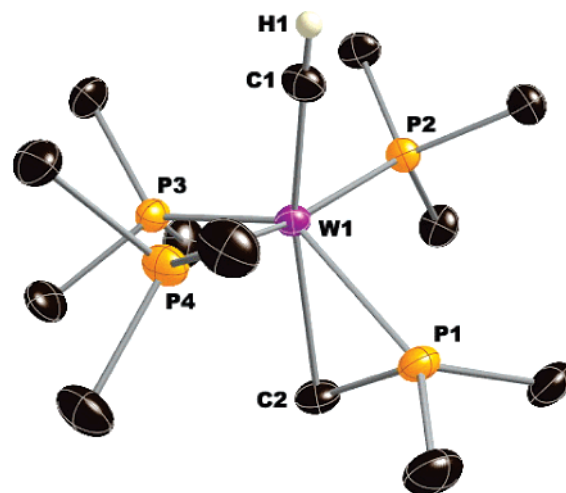


**Figure 6.** Crystalmaker depiction (50% probability thermal ellipsoids) of the molecular structure of **3**. H atoms, except the methylidyne H (arbitrary radius), are omitted for clarity. Selected bond lengths (Å): W1–C1, 1.814(5); W1–C2, 2.378(5); W1–P1, 2.3914(14); P1–C2, 1.767(6); W1–P2, 2.4353(13); W1–P3, 2.4361(16); W1–P4, 2.4377(14); C1–H1, 0.75(6). Selected bond angles (deg): C1–W1–P3, 106.65(19); C1–W1–P2, 84.69(17); C1–W1–P4, 84.68(16); C1–W1–P1, 121.15(19); C1–W1–C2, 164.6(2); P2–W1–P4, 169.30(4); P1–W1–P3, 132.20(5); C2–W1–P3, 88.71(14); C2–W1–P1, 43.49(14).

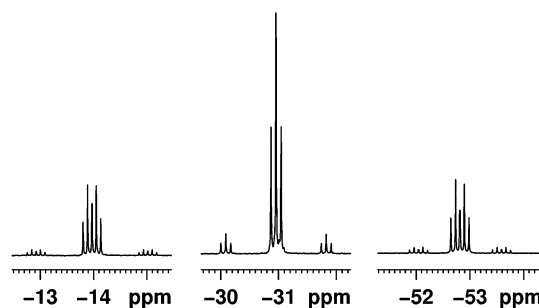


**Figure 7.**  $^{31}\text{P}\{^1\text{H}\}$  NMR spectrum of **3** in toluene- $d_8$  at 295 K.

attached to it and those attached to P2 and P4; obviously, the bond between P1 and C2 displaces these atoms from the normal octahedral sites. With regard to the  $\text{CH}_2\text{PMe}_2$  ligand, P1 is located “pseudo-cis” [angle C1–W1–P1 is 121.2(2)°] and C2 is located “pseudo-trans” [angle C1–W1–C2 is 164.6(2)°] relative to the methylidyne C1. The  $\text{W}\equiv\text{C}$  and  $\text{W}-\text{C}$  bond lengths are 1.814(5) and 2.378(5) Å, respectively, rather long for  $\text{W}\equiv\text{C}$  and  $\text{W}-\text{C}$  bonds, probably because of the strongly  $\sigma$ -donating nature of the opposing alkyl and methylidyne ligands. The constrained nature of the  $\text{CH}_2\text{PMe}_2$  ligand ameliorates this effect somewhat because these bonds are both shorter than the analogous bonds observed in  $(\text{dmpe})_2\text{W}(\text{t}^{\text{Bu}})\equiv\text{CH}$ , which are 1.827(5) and 2.405(6) Å, respectively.<sup>7b</sup> The bond between W1 and P1 must be quite strong, judging from the short bond length of 2.3914(14) Å, but also the average bond length of 2.436(1) Å of the other three  $\text{W}-\text{P}$  bonds is smaller than the 2.467(2) Å bond length found in **1a**. This shortening of the  $\text{W}-\text{P}$  bonds in **3** relative to **1a** can probably be attributed to a decrease in steric crowding in **3** due to the loss of the chloride ligand, allowing the phosphines to move closer to the W center.

The  $^{31}\text{P}\{^1\text{H}\}$  NMR spectrum (toluene- $d_8$ ; Figure 7) of **3** shows three resonances, all of them accompanied by W

(29) LDA as a reductant: (a) Ashby, E. C.; Mehdizadeh, A.; Keshpande, A. K. *J. Org. Chem.* **1996**, *61*, 1322. (b) Newkome, G. R.; Hager, D. C. *J. Org. Chem.* **1982**, *47*, 601. (c) Denny, W. A.; Herbert, J. M.; Woodgate, P. D. *Aust. J. Chem.* **1988**, *41*, 139. (d) Newkome, M.; Burchill, M. T. *J. Am. Chem. Soc.* **1984**, *106*, 8276.

(30) (a) Janak, K. E.; Tanski, J. M.; Churchill, D. G.; Parkin, G. J. *Am. Chem. Soc.* **2002**, *124*, 4182. (b) Baker, R. T.; Calabrese, J. C.; Harlow, R. L.; Williams, I. D. *Organometallics* **1993**, *12*, 830. (c) Cotton, F. A.; Cannich, J. M.; Luck, R. L.; Vidyasagar, K. *Organometallics* **1991**, *10*, 352. (d) Young, S. J.; Olmstead, M. M.; Knudsen, M. J.; Schore, N. E. *Organometallics* **1985**, *4*, 1432. (e) Chiu, K. W.; Howard, C. G.; Rzepa, H. S.; Sheppard, R. N.; Wilkinson, G.; Galas, A. M. R.; Hursthouse, M. B. *Polyhedron* **1982**, *1*, 441. (f) Karsch, H. H.; Klein, H.-F.; Schmidbaur, H. *Angew. Chem., Int. Ed. Engl.* **1975**, *14*, 637. (g) Werner, H.; Gotzig, J. *Organometallics* **1983**, *2*, 547. (h) Holland, A. W.; Bergman, R. G. *Organometallics* **2002**, *21*, 2149. (i) Harris, T. V.; Rathke, J. W.; Muetterties, E. L. *J. Am. Chem. Soc.* **1978**, *100*, 6966. (j) Werner, H.; Werner, R. J. *Organomet. Chem.* **1981**, *209*, C60. (k) Hajela, S.; Bercaw, J. E. *Organometallics* **1994**, *13*, 1147. (l) Chatt, J.; Davidson, J. M. *J. Chem. Soc.* **1965**, 843.

satellites. The doublet of triplets at  $-52.8$  ppm can be assigned to the  $\text{CH}_2\text{PMe}_2$  ligand, on the basis of  $^1\text{H}\{^{31}\text{P}\}$  NMR selective decoupling experiments. This assignment is supported by the fact that in related complexes containing both  $\text{CH}_2\text{PMe}_2$  and  $\text{PMe}_3$  ligands the highest-field  $^{31}\text{P}$  NMR resonance is usually assignable to the former ligand.<sup>31</sup> The  $C_s$  symmetry of **3** is indicated by the observation of one signal for the mutually trans  $\text{PMe}_3$  ligands at  $-30.7$  ppm. While this resonance appears to be a triplet, it is, in fact, a doublet of doublets with two nearly identical  $^2J_{\text{PP}}$  values of 13.5 and 14.0 Hz. The weak coupling between the P atoms of the  $\text{CH}_2\text{PMe}_2$  and the unique  $\text{PMe}_3$  ligand ( $^2J_{\text{PP}} = 26.5$  Hz) can be explained by a significantly bent P1–W1–P3 arrangement; an angle of  $132.20(5)^\circ$  was found in the solid state. It seems, therefore, that the structure of **3** in solution is similar to that in the solid state. Any appreciable exchange of the two types of  $\text{PMe}_3$  ligands does not occur because their  $^{31}\text{P}$  (and  $^1\text{H}$ ) NMR resonances do not coalesce up to a temperature of 370 K. The static nature of **3** contrasts with the dynamic behavior of the tungsten(II) hydride  $\text{WH}(\text{PMe}_3)_4(\text{CH}_2\text{PMe}_2)$ ,<sup>31b</sup> which displays temperature-dependent NMR spectra. At elevated temperatures, decomposition of **3** is significant, as free  $\text{PMe}_3$  becomes visible in the  $^1\text{H}$  and  $^{31}\text{P}$  NMR spectra and a dark-gray material is deposited on the wall of the NMR tube.

In the  $^1\text{H}$  NMR spectrum, the methylidyne and methylene protons are located at 8.61 and  $-1.33$  ppm, respectively, as first-order multiplets due to coupling to the P nuclei as well as to each other ( $^4J_{\text{HH}} = 0.9$  Hz). The methylidyne C–H coupling constant  $^1J_{\text{CH}}$  was measured directly from the  $^1\text{H}$  NMR spectrum of  $^{13}\text{C}$ **3** and is only 125 Hz, even lower than the already low value of 132 Hz for  $^{13}\text{C}$ **1a**. The aliphatic region of the spectrum consists of a doublet of doublets for the  $\text{CH}_2\text{PMe}_2$  group, a doublet for the unique  $\text{PMe}_3$  ligand, and a virtual triplet<sup>32</sup> for the two mutually trans  $\text{PMe}_3$  ligands. Upon cooling of the sample, broadening of the latter resonance occurs, and at ca. 200 K, it is split into two broad signals in a 2:1 ratio. Further cooling to 185 K splits the largest of the two resonances into two, so that a

1:1:1 ratio of broad resonances at 1.83, 1.74, and 1.09 ppm, each integrating to six protons, is finally obtained. We attribute this low-temperature behavior to a slow (on the NMR time scale) rate of rotation around the W–P bonds of the mutually trans  $\text{PMe}_3$  groups, thereby placing the methyl groups on each  $\text{PMe}_3$  ligand in three chemically distinct positions. It is very well possible that the strong W d–(P–C)  $\sigma^*$  back-bond, which is of  $\pi$  symmetry, is the reason for the slow rotation.

Although **1b** also undergoes deprotonation to afford a product that appears to be similar to **3**, we have been unable to obtain it in pure form. The reaction proceeds only very slowly with LDA, while with KBN a significant amount of  $(\text{dmpc})_2\text{W}(\text{CH}_2\text{Ph})\equiv\text{CH}$  is formed by nucleophilic substitution of the chloride ligand. NMR spectroscopy indicates that the methyl (as opposed to the methylene) group is deprotonated and, as expected, there are no symmetry elements left in the product. For example, there are four resonances in the  $^{31}\text{P}\{^1\text{H}\}$  NMR spectrum and seven distinct methyl resonances in the  $^1\text{H}$  NMR spectrum, and the two W– $\text{CH}_2$  protons are diastereotopic.

## Conclusions

One-electron oxidation of the classical Schrock methylidyne using the trityl cation as the oxidant occurs smoothly to give the cationic methylidyne compounds **2**, the first monomeric d<sup>1</sup> methylidyne. X-ray data and ESR spectroscopy indicate that the single electron is largely accommodated in a metal-based orbital, perhaps offering a rationale for the stability of these species as monomers rather than dimers. Attempts to deprotonate the compounds invariably led to one-electron reduction with the bases employed, but the neutral methylidyne complex **1a** so produced was deprotonated by further base at one of the  $\text{Me}_3\text{P}$  ligands.

**Acknowledgment.** Funding for this work came from the Natural Sciences and Engineering Research Council of Canada in the form of a Discovery Grant (to W.E.P.) and the Alberta Ingenuity Fund in the form of a Studentship (to E.F.v.d.E.). The authors thank Prof. Michael Hopkins (Chicago) for useful discussions.

**Supporting Information Available:** Crystallographic data (CIF) for **2a**· $\text{C}_6\text{D}_6$ , **2b**, and **3**. This material is available free of charge via the Internet at <http://pubs.acs.org>.

IC0611342

(31) (a) Gibson, V. C.; Grebenik, P.; Green, M. L. H. *J. Chem. Soc., Chem. Commun.* **1983**, 1101. (b) Gibson, V. C.; Graimann, C. E.; Hare, P. M.; Green, M. L. H.; Bandy, J. A.; Grebenik, P. D.; Prout, K. *J. Chem. Soc., Dalton Trans.* **1985**, 2025. (c) Wenzel, T. T.; Bergman, R. G. *J. Am. Chem. Soc.* **1986**, *108*, 4856. (d) Mainz, V. V.; Andersen, R. A. *Organometallics* **1984**, *3*, 675.

(32) Harris, R. K. *Can. J. Chem.* **1964**, *42*, 2275.